Eurographics/ IEEE-VGTC Symposium on Visualization 2009
H.-C. Hege, I. Hotz, and T. Munzner
(Guest Editors)

Volume 28 (2009), Number 3

Lifted Domain Coloring

Konstantin Poelke[†] and Konrad Polthier[†]

Freie Universität Berlin, Germany

Abstract

Complex-valued functions are fundamental objects in complex analysis, algebra, differential geometry and in many other areas such as numerical mathematics and physics. Visualizing complex functions is a non-trivial task since maps between two-dimensional spaces are involved whose graph would be an unhandy submanifold in four-dimensional space. The present paper improves the technique of "domain coloring" in several aspects: First, we lift domain coloring from the complex plane to branched Riemann surfaces, which are essentially the correct domain for most complex functions. Second, we extend domain coloring to the visualization of general 2-valued maps on surfaces. As an application of such general maps we visualize the Gauss map of surfaces as domain colored plots and establish a link to current surface parametrization techniques and texture maps. Third, we adjust the color pattern in domain and in image space to produce higher quality domain colorings. The new color schemes specifically enhance the display of singularities, symmetries and path integrals, and give better qualitative measures of the complex map.

Categories and Subject Descriptors (according to ACM CCS): Applications [Computer Graphics]: Visualization in Mathematics, Illustrative Visualization, Complex Functions, Riemann Surfaces—

1. Introduction and Related Work

Even today, visualizing complex functions is a tricky task, mostly due to dimensional reasons. In geometry and differential calculus of real variables, we are used to imagine real valued functions as graphs over a domain, which is often part of the Euclidean space or more general a submanifold, e.g. a surface in $\mathbb{R}^3$. Unfortunately, this does not work even for functions $f : \mathbb{R}^2 \to \mathbb{R}^2$ and therefore not for complex functions $f : \mathbb{C} \to \mathbb{C}$, so one has to look for other techniques visualizing these functions. The most intuitive way is probably examining separately the domain and the range of the function, e.g. one can examine grid transformations induced by the function. An alternative may be treating the modulus or the argument as a real valued function and plotting its graph over a domain $U \subset \mathbb{C} \cong \mathbb{R}^2$, but this would only reflect one property, as it is kind of a dimension reduction and does not describe the function as a whole. Farris [Far] introduced a technique known as "domain coloring", which plots a function right onto the domain. In this paper, we extend this technique by the following points:

- We introduce Riemann surfaces as appropriate domains and color them in order to get an entire understanding of multivalued functions.
- We transfer the method of domain coloring to arbitrary parametrized surfaces in $\mathbb{R}^3$ by examining their corresponding Gauss maps.
- Based on the established domain coloring techniques, we provide a coloring holding "indicators" allowing us to get a detailed impression of a function's behavior and generate insightful, high-quality plots.

The term "domain coloring" has been coined by Farris [Far], who uses simple color gradients without further features. The plots of Pergler [Per] and Lima da Silva [dS] are of better quality, but still lack some important information, e.g. they do not provide any information about distorsion or conformality. Lundmark [Lun04] gives a detailed introduction and uses a color scheme revealing several important aspects of complex functions. In particular, he plots a grid in order

[†] Supported by DFG Research Center MATHEON "Mathematics for key technologies"

to detect non-conformal points. Hlavacek [Hla] provides a gallery of complex function plots, using color schemes similar to Lundmark's and Pergler's.

2. Improving Domain Coloring

To begin with, we explain briefly the established method of domain coloring. Domain coloring, as the name suggests, makes use of a color spectrum to compensate the missing dimension. More precisely, we discard the approach of plotting the function somehow on an independent axis (as we would do when we plot the modulus over the domain, for instance), but plot it right onto the domain, i.e. we color the domain in a particular way. Now, the effectiveness and flexibility of domain coloring lies in the choice of an adequate reference color scheme. In the general case, we are given a function $f : U \to V$ with two sets U, V, e.g. manifolds, and choose a coloring $col : V \to HSB$, where HSB denotes the HSB color space. Then, for any $z \in U$ we compute $f(z)$, evaluate $col(f(z))$ and assign the resulting color to the preimage z. When we are done, we have a colored domain where at each point the color tells us where this point gets mapped to. Since the HSB space is closely related to polar coordinates on the solid sphere $B_1 = \{r(\cos\varphi\cos\theta, \cos\varphi\sin\theta, \sin\varphi) | 0 \le r \le 1\}$ (hue can be easily associated with θ, saturation with r and brightness with φ), it makes good sense to decompose col into $col = c \circ p$ with $c : B_1 \to HSB$, $p : V \to B_1$. In classic domain coloring, one has $U \subset \mathbb{C}, V \subset \overline{\mathbb{C}}$ (where $\overline{\mathbb{C}} := \mathbb{C} \cup \{\infty\}$ and p can be chosen to be the inverse stereographic projection, for instance. Using our more general setting, we cannot only extend the coloring to Riemann surfaces U, which are the true domains of complex functions, but to arbitrary maps, e.g. parametrized regular surfaces $V \subset \mathbb{R}^3$. In a way, the choice of p then determines the characteristics of f, which are carried to the color space, see section 7 for examples.

In the following, we want the mapping c to be such that the south pole of B_1 gets mapped to black, the equator to fully saturated and brightened colors and the north pole to pure white. If p is the inverse stereographic projection, this corresponds to zero being black and infinity being white. This gives us an idea on how to define saturation and brightness values. Furthermore, we like to preserve the canonical hue-argument relation and obtain a continuous color gradient passing through the whole hue spectrum, as can be seen in figures 1 and 2.

So far, we are able to detect stationary points (zeros and poles) of a given function and the qualitative distortion of the domain: comparing the colors of the plot with the corresponding points of the reference coloring gives us a hint of how the argument has changed. Another property of some interest is in general the direction of growth of the function's modulus, as the spots denoting zeros and poles give only a very coarse impression. (It is understood that the modulus will grow between a zero and a pole.) Referring to Lundmark, it is a good idea to display some elements helping you to keep track of the growth. This is done by blending the color plot with semi-transparent, repeated rings whose gradients go from dark to bright, representing the direction of growth. By taking the fractional part of the logarithm of the modulus, we obtain a value between 0 and 1 which we use as the ring's brightness. Note that by taking the logarithm, we assure a quite regular behavior of these rings around poles. However, the exponential map counteracts the logarithm and one surely can imagine functions whose growth is so strong that even the logarithm cannot keep the modulus under control. This is a general problem of coloring schemes which work pointwise and do not treat the function as a whole. At least, the important class of meromorphic functions can be tackled this way and one is free to choose an adequate basis of the logarithm, depending on the maximal pole order of f.

As one of our contributions, we add k rays starting at zero and running through the k-th unit roots in order to get a feeling of the distortion induced by f. By doing this, we divide our domain into k equally sized segments. Therefore, by comparison with the colored range of f, we get an impression which regions get compressed or stretched by f and which ones are reasonably maintained.

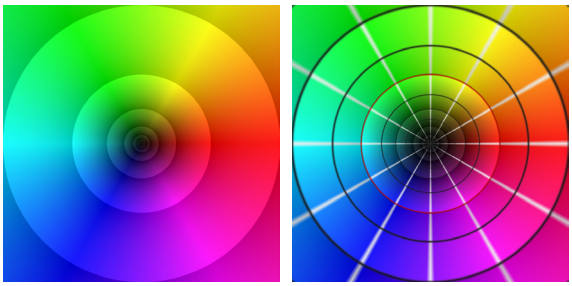

(a) Growth indicators (b) The reference coloring

Figure 1: Indicators of our reference coloring

In a way, each ray is a shortest connection between zero and infinity. Hence, following a gray line in the picture above from a zero to a pole means following a most steeply rising path of the modulus. More precisely, if $z = x + iy$, then we follow the gradient $\nabla |f|_{z=x+iy} = (\partial_x |f(z)|, \partial_y |f(z)|)$, which points into the direction of the most steepest ascent. Thus, we can carefully predict the relief of a function without explicitly plotting its modulus as a graph over a two-dimensional domain.

Having introduced radial lines, now it is obvious to add concentric circles, yielding a kind of a polar grid blended over the reference coloring, which is in a way the canonical grid one can lay onto the Riemann sphere. When circling around such a contour (or level) line, the modulus is constant. The contour gives you another hint on how to imagine a complex function: similarly to the circles representing the direction of growth, the level lines tell you about the growth behavior in every direction. If these lines are nested circles

sharing the same center, then one observes a (locally) uniform increase or decrease of the function's modulus. Note that if f is meromorphic, every closed contour line contains at least one zero or pole in its interior. In particular, if many contour lines concentrate around a point z_0, then z_0 is either a (multiple) zero or a pole. This observation is known as the "maximum principle" and plays a decisive role in the study of PDEs.

Keep in mind that in the reference coloring the radial lines intersect each level line in a right angle. We will refer to this observation below. The following plots of the next sections use the coloring shown in figure 1b (we chose the rays to run through the 12th unit roots). For better orientation, we have highlighted the unit circle. This coloring now offers a rich

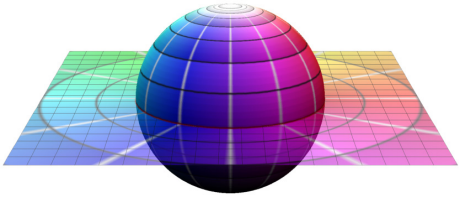

Figure 2: Our reference coloring on the Riemann sphere

set of characteristics we will benefit from in the following, and we will obtain more detailed, informative plots than any previous works provide. Yet, in some cases one may want to emphasize certain aspects of a function by adjusting the coloring. We will make use of this option in the section about the reflection principle.

3. Interpreting Domain Colored Plots

In the following we provide hints how to read domain colored plots. As an example, we consider the meromorphic function $f_1 : [-3,3] \times [-3i,3i] \to \overline{\mathbb{C}}$ defined by $f_1(z) = \frac{(z-1)(z+1)^2}{(z+i)(z-i)^2}$, inducing the plot in figure 3.

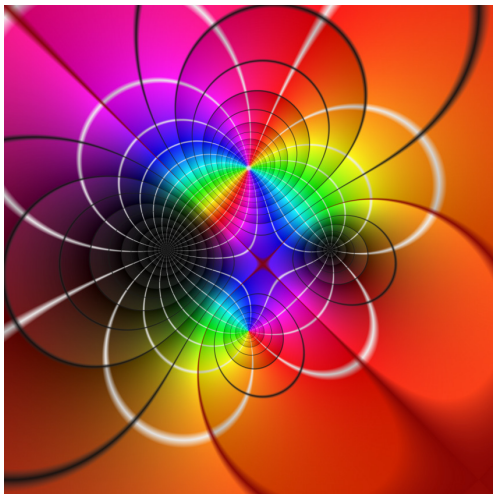

Figure 3: Plot of the rational function f_1

3.1. Deformation

Take a close look at the colors and compare them with figure 1b. Note that the center of the picture is colored in blue and magenta colors, thus by comparison to the original color map, this region gets mapped somewhere onto the lower left half plane. Now, consider the margin of the plot. Except for the upper left corner, it is mostly colored in orange or ginger, so this region gets mapped onto the upper right plane with the real parts of the function values dominating the imaginary parts (for it is more red then yellow-green).

3.2. Zeros and Poles

Obviously, this function has two zeros, one at $+1$, the other one at -1. Due to the choice of our coloring, zeros are colored as black spots, so you can easily detect them on the plot. More generally, a point z with $|z| < 1$ gets darker the more $|z|$ approaches zero, thus one has a continuous color gradient from points with $|z| = 0$ to those with $|z| = 1$, being black at the stationary value $|z| = 0$ and reaching its full color intensity at $|z| = 1$. Having a multiple zero z_0 means that this gradient emphasizes the almost black regions and as a result, the dark neighborhood grows larger. Thus, the higher the multiplicity of a zero is, the larger is the extension of the black spot.

Consider a simple zero, e.g. $z = 0$ under the identity map. You observe, that you pass through the whole color spectrum when you circle around 0 once if your function is holomorphic in a neighborhood containing the zero. Now, have a look at both the zeros of our example 3: The right one is a simple zero, so when you circle around it, you get the whole spectrum once. However, the left one is a double zero and you find that when you circle around -1, you run through the color spectrum twice. This is just reasonable and generalizes to multiple zeros such as $(z-a)^k$. For example, take the monomial $z \mapsto z^k$ and consider a point $w = re^{i\phi} \neq 0$, then it gets mapped to $r^k e^{ik\phi}$, in particular, the argument gets multiplied by k. But this represents exactly the behavior of the colored plot: All points on the line $\mathbb{R}^+ \cdot e^{i\frac{2\pi}{k}}$ get already mapped to the positive real axis, therefore, circling once around 0 means circling k times around 0 in the complex plane—the power k somehow "overlays" the complex plane k times with itself.

Pretty much the same observations hold true for singularities: Consider a simple pole, e.g. $z_0 = 0$ under $z \mapsto \frac{1}{z}$ (see figure 6a). This mapping is also known as "inversion" and mirrors the complex plane at the real axis. This can be seen best when considering a point $w = re^{i\phi} \neq 0$, then $\frac{1}{w} = \frac{1}{r}e^{-i\phi}$. As a result, when circling around 0 counterclockwise, you run through the color spectrum clockwise, so the "orientation" of the spectrum has switched. This behavior can be extended to multiple poles as well and again one obtains—besides the changed orientation—a k-times overlaying of the plane onto itself.

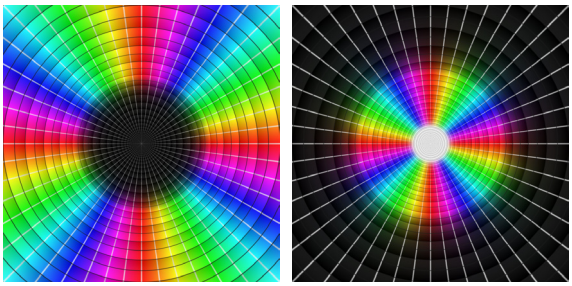

(a) Multiple zero (b) Multiple pole

Figure 4: Typical pattern of a multiple zero z^k and a multiple pole z^{-k}

More generally, let f be a function which has a pole of order k in z_0 and is holomorphic in a neighborhood of z_0, then its Laurent series looks like

$$f(z) = \frac{a_{-k}}{(z-z_0)^k} + \cdots + \frac{a_{-1}}{z-z_0} + \sum_{n=0}^{\infty} a_n (z-z_0)^n$$
$$= \frac{1}{(z-z_0)^k} g(z)$$

with a holomorphic function $g(z)$ with $g(z_0) = a_{-k} \neq 0$. With this in mind, all functions having a $k-$pole in z_0 look the same, up to multiplication by a constant $a_{-k} \in \mathbb{C}$, i.e. rotation and dilation of the surrounding region. Figure 4 compares the functions $z \mapsto z^k$ and $z \mapsto z^{-k}$ for $k = 4$.

3.3. Conformality

An important property of holomorphic functions is their (local) conformality in regions with non-vanishing derivative, i.e. they preserve angles between any two curves intersecting each other (of course, holomorphic functions with non-vanishing derivative are conformal by definition, as the Jacobian, considered as a 2×2-matrix over $\mathbb{R}$, is a scaled rotation matrix). As a result, the radial rays intersect the contour lines in a right angle both in the domain and in the image, except for points in which the derivative vanishes. A quick calculation yields

$$\frac{d}{dz} f_1(z) = \frac{(z+1)^2 + 2(z^2-1)}{(z-i)^2(z+i)} - \frac{2(z-1)(z+1)^2}{(z-i)^3(z+i)} - \frac{(z-1)(z+1)^2}{(z-i)^2(z+i)^2} \quad (1)$$

and

$$\frac{d}{dz} f_1(z) = 0 \Leftrightarrow z_{1,2,3} = -1, \frac{3-\sqrt{7}}{2} + \frac{\sqrt{7}-3}{2} i, \frac{3+\sqrt{7}}{2} - \frac{3+\sqrt{7}}{2} i. \quad (2)$$

These are the critical points in which our function is not conformal. It is not surprising that one point is the double zero, for one can easily see that the number of lines leaving the black spot has doubled. The second one is close to the origin, at about $0.177 - 0.177i$. You can detect this point as an intersection of two reddish lines, both of them denoting the unit circle, which of course does not intersect itself in the reference coloring. Thus, in this point you can clearly recognize the corruption of the angle. The same observation holds for the last non-conformal point in the lower right corner.

3.4. Essential Singularities

To a certain extent, the type of singularities discussed above possess a fairly regular behavior. That is to say, the neighborhood of such a singularity is the "very outer" ring of the $k-$times overlaid, inverted complex plane. Note that in the canonical topology of the Riemann sphere, a neighborhood of a singularity is usually defined as $B_\varepsilon(\infty) = \left\{ z \in \mathbb{C} : Abs(z) > \varepsilon^{-1} \right\}$, so the "very outer" ring can be informally understood to be $B_{\varepsilon \approx 0}(\infty)$. We now discuss so-called essential singularities, whose behaviour in their neighborhood is completely different to the "nonessential" ones. In fact, they show a strong oscillation and seem to consistently hit the whole sphere. This lax observation has been

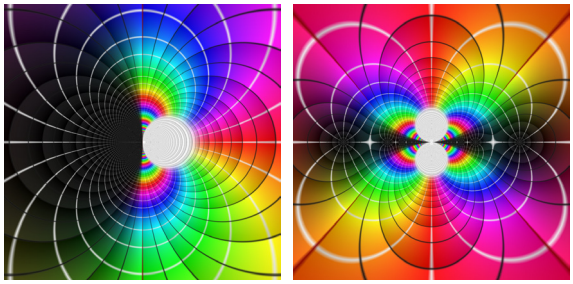

(a) $f(z) = \exp(z^{-1})$ (b) $f(z) = z\sin(z^{-1})$

Figure 5: Essential singularities

made precise by C.E. Picard:

Theorem 1 (Picard) Let $U \in \mathbb{C}$ be an open set, $z_0 \in U$ and let $f : U \setminus \{z_0\} \to \mathbb{C}$ be a holomorphic function with an essential singularity in z_0. Then, $f(U \setminus \{z_0\}) = \mathbb{C}$ or $f(U \setminus \{z_0\}) = \mathbb{C} \setminus \{w\}$ for a single point $w \in \mathbb{C}$.

The theorem states that every neighborhood of z_0, no matter how tiny it is, gets mapped to almost the whole complex plane. We can recover this property in figure 5 depicting the function $f(z) := \exp\left(z^{-1}\right)$ and the—in a sense—related function $f(z) := z\sin(z^{-1})$, both defined on $[-0.5, 0.5] \times [-0.5i, 0.5i]$. Approaching zero from the positive real axis results in large values whereas approaching from the negative real axis results in almost zero values. The interesting part lies in between, i.e. if we approach zero on the imaginary axis, we streak past the whole complex plane: near the domain zero we have the functions "almost-zero" to the left (the black blob) and infinity to the right (the white blob). In between we circle around the complex plane again and again (this is the "oscillation"). Hence, a function's acting close to an essential singularity strongly depends on the direction from which it approaches the singularity point. This

observation stands in stark contrast to the quite regular behavior around poles and brings out the qualitative difference between essential and nonessential singularities.

4. Path Integrals

A frequent question in complex analysis is whether a closed curve integral of a given function around a point z_0 vanishes or not. A fundamental answer was given by A.L. Cauchy in his famous integral theorem giving rise to numerous other important theorems in complex analysis. Our plots give us some hints whether an integral might vanish or not. Therefore let us consider once more the inversion $z \mapsto z^{-1}$ on $[-1,1] \times [-i,i]$ and discuss the path integral over the curve $\gamma(t) = e^{it}$ defined on $[0, 2\pi]$, which is

$$\oint_\gamma \frac{1}{\zeta} d\zeta = 2\pi i.$$

Following the descriptive approach of Needham [Nee97], we approximate the curve integral by a Riemann sum and obtain

$$\oint_\gamma f(\zeta)d\zeta = \int_0^{2\pi} f(\gamma(t))\gamma'(t)dt \approx \sum_i f(\gamma(\tilde{t}_i))(\gamma(t_{i+1}) - \gamma(t_i))$$

for a partition $0 = t_0 < t_1 < \cdots < t_n = 2\pi$ with sample points $\tilde{t}_i \in (t_i, t_{i+1})$. If γ is rectifiable (which holds true for our particular γ defined above), the Riemann sum converges to the path integral for $n \to \infty$, i.e. $dt_i := t_{i+1} - t_i \to 0$ resp. $\Delta_i := \gamma(t_{i+1}) - \gamma(t_i) \to 0$. To simplify the procedure, we assume all dt_i (and hence all Δ_i to be equal distant, i.e. $\forall i : dt = dt_i$. Now, recall that a multiplication of Δ_i with a complex number $f(\gamma(\tilde{t}_i))$ can be interpreted as a rotation and scaling of the vector Δ_i. If we add the Δ_i as oriented arrows to the plot, we can easily imagine the transformation of them. Figure 6a shows the sample points $\tilde{t}_i$ which were chosen, such that $\gamma(\tilde{t}_i)$ are the 8th unit roots and $\tilde{t}_i = (t_{i+1} - t_i)/2$ (one has to adjust the parameter interval, here $t_k = (2k-1)\pi/8$ mod 2π for $k = 0, \ldots, 8$), together with the corresponding Δ_i-arrows. In the following, we number the Δ_i counterclockwise, beginning with Δ_1 being the arrow crossing the positive real axis.

The sample point for Δ_1 is the intersection of the red radial line with the unit circle denoting 1 and therefore $f(\gamma(\tilde{t}_1)) = 1$, so Δ_1 remains untouched. Δ_3 has its corresponding sample point at the intersection of the unit circle with the violet-blue radial line, which stands for $-i$. Thus Δ_3 is rotated by 90° clockwise and now points upwards as well. $\gamma(\tilde{t}_5)$ is the cyan -1 and $\gamma(\tilde{t}_7)$ is the light-green i. Hence, after multiplication Δ_5 and Δ_7 are pointing upwards, too. The color gradient between these characteristic points tells us, that finally all the arrows have no other choice than pointing upwards and hence the sum cannot vanish, for the arrows do not cancel each other. Figure 6b demonstrates this situation. Clearly, this observation holds true for every discretization and even for the limit $n \to \infty, dt \to 0$, where the arrows shrink to points. We can imagine these points having somehow a "momentum" which is given by $\gamma'(t)$. Then, at each point, the underlying color tells us how the momentum is changed by the function. In our example, the function counteracts the direction of the momentum (but does not change its value) exactly by the angle the momentum has, and we accumulate all momenta γ pointing in the upper imaginary direction. When we have circled around γ, we have gathered a total amount of 2π, pointing into the direction i, and the resulting value $2\pi i$ is understandable.

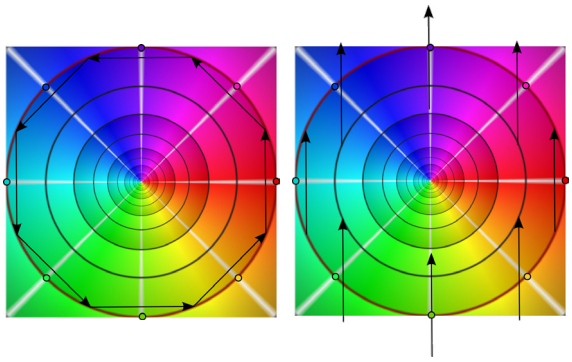

(a) Δ_i depicted as arrows. The small spots on the rays denote the sample points $\gamma(\tilde{t}_i)$

(b) All arrows are twisted by the function

Figure 6: Inversion acting on "momentum"

In general it is hard to tell if all arrows are pointing exactly in the same direction and in most cases it is impossible to predict a quantitative outcome. Nevertheless, one will often find that they are at least all pointing in the same half-plane, which suffices to conclude that the path integral does not vanish.

5. Further Examples

5.1. Unit Roots

We consider the polynomials of type $f_2(z) := z^n - 1$ resp. $f_3(z) := z^{-n} - 1$, whose zeros are exactly the n-th unit roots $\exp(2\pi ik/n)$ for $k = 0, \ldots, n-1$. (These polynomials are of high importance in algebra, for instance in the theory of field extensions.) For z with $Abs(z)$ large, we expect them to behave similarly to $z \mapsto z^n$ resp. -1, since in the first case, -1 has almost no effect whereas in the second case, z^{-n} has almost no effect. This can be seen in figure 7, using $n = 5$ on $[-2,2] \times [-2i, 2i]$.

f_2 is cyan in the interior of the unit circle, which indicates complex numbers with negative real values and almost zero imaginary part. Furthermore, outside the unit circle you find a coloring which more and more equals the coloring of $z \mapsto z^5$, the more you move away from the origin. The curves meeting in the origin all get mapped onto the unit level line with radius 1 (Note $Abs(f_2(0)) = 1$), indicating a breach of conformality.

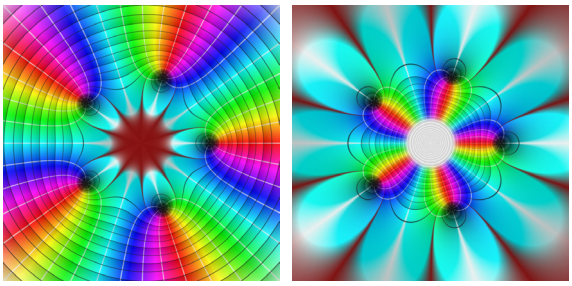

(a) f_2 (b) f_3

Figure 7: Unit roots of $f_2(z) = z^5 - 1$ (left) and $f_3(z) = z^{-5} - 1$

The white rays pointing outwards in the plot of f_3 depict exactly the negatives real axis and the complete region outside the unit circle (which passes through the five black spots) is colored cyan. Note that in the corners, the image is dominated by a blurring bordered by reddish-brown lines. These lines get mapped onto the unit circle (which in particular crosses -1), each of them circling around a zero at a unit root; since the wide-stretched blurring indicates values whose modulus is almost 1, this observation exactly comes up to our expectations.

5.2. Schwarz Reflection Principle

Holomorphic functions defined on certain subsets of open connected sets D which are symmetric with respect to the real axis can be extended to holomorphic functions on the entire set D. The Schwarz reflection principle states this fact more precisely:

Theorem 2 (Schwarz Reflection Principle) Let $D \subset \mathbb{C}$ be an open, connected, non-empty set, which is symmetric to the real axis, i.e. $z \in D \Rightarrow \bar{z} \in D$ and $D_+ := \{z \in D | Im(z) > 0\}$, $D_- := \{z \in D | Im(z) < 0\}$, $D_0 := \{z \in D | Im(z) = 0\}$. If f is continuous on $D_+ \cup D_0$, holomorphic on D_+ and $f(D_0) \subset \mathbb{R}$, then it has a holomorphic continuation on D_- and $f(z) = \overline{f(\bar{z})}$.

Have a look at the example functions depicted in figures 8a and 8b. The first one, also known as "Joukowski function", is holomorphic on $\mathbb{C} \setminus \{\pm i\}$, the second one on $\mathbb{C} \setminus \{0\}$. Furthermore, it is clear that for both functions it is $f(\mathbb{R}) \subset \mathbb{R}$ resp. $f(\mathbb{R} \setminus \{0\}) \subset \mathbb{R}$. Thus, they satisfy the requirements of Schwarz' theorem and have a holomorphic continuation onto the lower half plane (which is unique by the identity theorem). Figures 8c and 8d show the same functions, this time using a gradient which is symmetric to the real axis. Note, that although we are losing most information about the argument, the symmetry property is easier to recognize. So, in general it is a good idea to choose the color scheme according to the properties one wants to accentuate. Nevertheless, our reference coloring in 1b does a good job as an all-round coloring

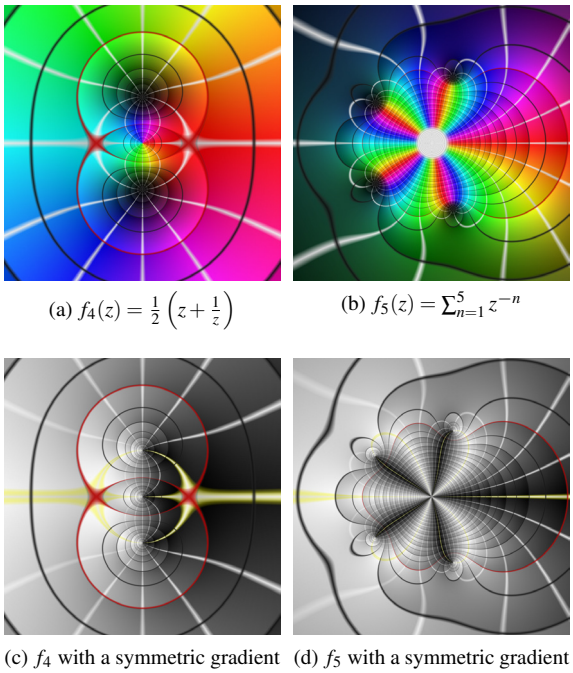

(a) $f_4(z) = \frac{1}{2}\left(z + \frac{1}{z}\right)$ (b) $f_5(z) = \sum_{n=1}^{5} z^{-n}$

(c) f_4 with a symmetric gradient (d) f_5 with a symmetric gradient

Figure 8: Visualizing the Schwarz reflection principle

5.3. Elliptic Functions

By coloring the domain of elliptic functions, we obtain patterns repeating in real and imaginary direction, which is due to the double periodicity of these functions. Figure 9 shows the well-known Weierstrass $\wp$-function with parameters $\omega_1 = 1, \omega_2 = \tau$ for $\tau = 0.5 + 0.5i$ and $\tau = 0.2 + 0.8i$. One can clearly recognize the deformation of the underlying grid $\Lambda = \mathbb{Z} + \tau\mathbb{Z}$.

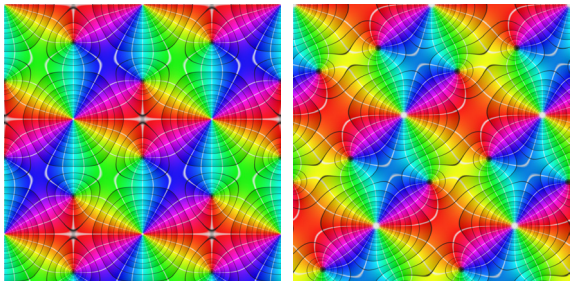

(a) $\wp$-function, $\tau = 0.5 + 0.5i$ (b) $\wp$-function, $\tau = 0.2 + 0.8i$

Figure 9: Weierstrass $\wp$-functions

6. Lifting Domain Coloring to Riemann Surfaces - Coloring of Multivalued Functions

So far, coloring the domain in $\mathbb{C}$ has worked properly. Nonetheless, for many functions the method discussed above fails in revealing essential properties; their domain somehow does not fit into the topology of the complex plane. For instance, consider the functions $f_6(z) := \sqrt{z}$, $f_7(z) := \log z$

(the principal branch) and $f_8(z) := \sqrt{z+1}\sqrt{z-1}$ defined on $[-3,3] \times [-3i,3i]$. In the first two cases, the color gradient has a discontinuity at the positive real axis, in the third case, it has a discontinuity between -1 and $+1$. Figure 10 depicts the situation. This problem occurs in general when we con-

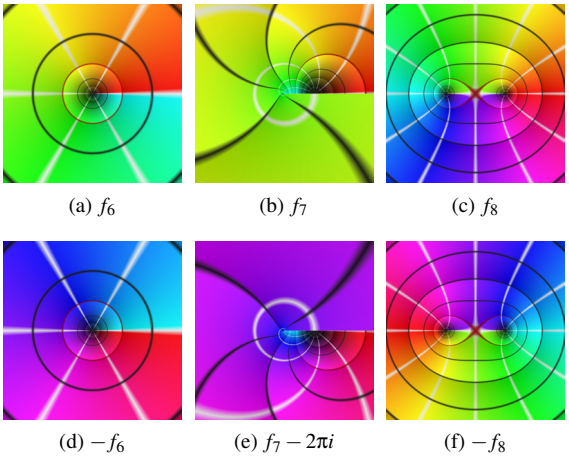

(a) f_6 (b) f_7 (c) f_8

(d) $-f_6$ (e) $f_7 - 2\pi i$ (f) $-f_8$

Figure 10: Discontinuity arising from square roots (f_6, f_8) and logarithms (f_7)

sider inverse functions of non-injective functions, for they are multi-valued. As a consequence, now there are several colors, according to the multiple values, getting assigned to a single point in the preimage. Hence we do not consider its domain to be nested in the complex plane, but allow a Riemann surface to serve as a domain of the function. In particular, the domain is allowed to possess a couple of layers, the “branches”, corresponding to the number of distinct values the function takes for a single point. Figure 11a and 11b show a model for the Riemann surface of the square root function f_6. The advantage of having a second layer allows to resolve the discontinuity by switching to the other layer when passing over the branch cut.

Although the color plot of the logarithm in figure 10b looks quite similar to the plot of the square root (the branch cut is the positive real axis), its overall behaviour is of a different kind. Figure 10e demonstrates that the discontinuity cannot be resolved by just introducing a second layer; of course we could connect the reddish part of 10b with the reddish part of 10e as we have done in 11b, but a new discontinuity would arise if we connected the green edge of 10b with the magenta edge of 10e. Instead, the correct model is an inifite "spiral stair" as shown in figure 11c. In fact, the fundamental reason of roots not being injective is the periodicity of the exponential map and the resulting non-injectivity of the logarithm. Whereas the equation $z^2 = w$ has only two solutions, $\exp(z) = w$ has inifitely many solutions (if z_0 is a solution, so is $z_0 + k2\pi i$ for all $k \in \mathbb{Z}$). As a consequence, the surface for f_6 has only two layers whereas the surface for f_7 has infinitely many different layers. That is why speaking of a “branch” of the logarithm is an illustrative formulation.

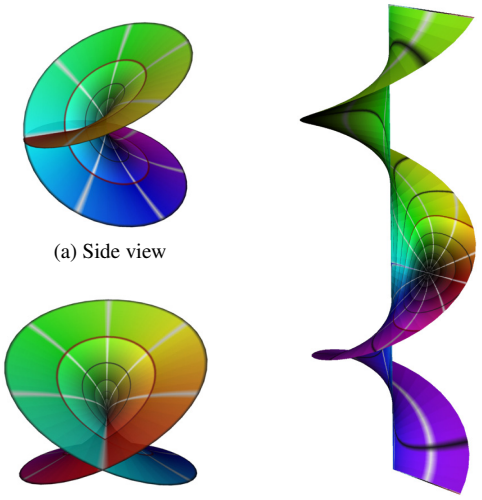

(a) Side view

(b) Front View

(c) 2 levels of the infinite "spiral stair”

Figure 11: Riemann surfaces for $\sqrt{z}$ and $\log(z)$

Figure 12 shows a more complicated example representing a Riemann surface for f_8. This time, the branch points

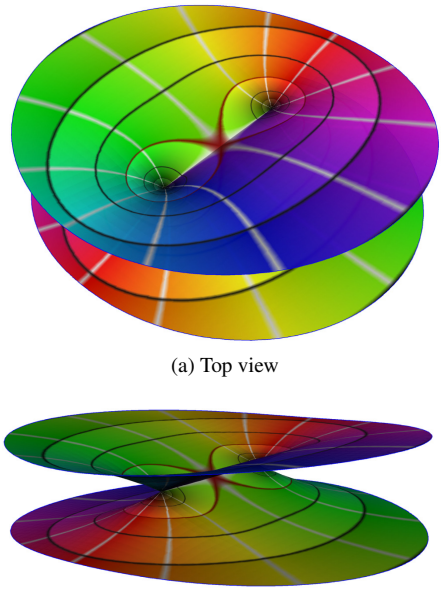

(a) Top view

(b) Side view

Figure 12: Riemann surface for f_8

are -1 and 1. By circling around one of these points, one ends up on the other layer in order to preserve continuity. Another round will bring us back to the layer where we have started. Note that it is also possible to go "downstairs” at one point and "upstairs” at the other point, in contrast to the previous square root example, which provides only one path. In a way, each branch point is kind of a separate gate to another layer enabling us to walk continuously through the range of the function.

7. Coloring Parametrized Surfaces

Finally, we extend domain coloring to general parametrized surfaces in $\mathbb{R}^3$. In the following, we require such a surface to be regular, so that it has a well-defined Gauss map everywhere. Studying the normal vector gives in general a fairly good aggregation of the characteristic properties of the surface, most of which are determined by curvature, e.g. principal curvature directions, so we choose p to be the Gauss map. Probably the most easily accessible surfaces are those which can be written as function graphs over the domain itself, i.e. surfaces of the type $(u,v) \mapsto (u,v,f(u,v))$. Figures 13a-13f display some exemplary function graphs and their Gauss maps. You can easily detect stationary points as before. Note that the level lines correspond to circles of latitude on the Riemann sphere whereas the radial rays denote the circles of longitude. Figure 13g depicts the Gauss map of the Möbius strip parametrized as

$$[0,2\pi] \times [-1,1] \ni (u,v) \mapsto \frac{1}{2} \begin{pmatrix} \cos(u)\,(2+\cos(u/2)\,v) \\ \sin(u)\,(2+\cos(u/2)\,v) \\ \sin(u/2)\,v \end{pmatrix}$$

Referring to our previously observated relations to Riemann surfaces, one notices the Gauss map of the Möbius strip has a period of 4π. In a way, this behavior is similar to the square root discussed above, which shows a discontinuity when circling around the complex plane once (we managed this problem by switching to another layer). Here, we have a discontinuity of the normal when circling just once, and we have to do it twice in order to restore a continuous normal transition.

8. Conclusion

We have generalized the technique of domain coloring to multivalued functions, whose ambiguity can be resolved by considering Riemann surfaces as their actual domains. However, domain coloring does not restrict to complex valued functions, as we have seen above: by using an adequate projection onto the Riemann sphere, one can easily extend the method in order to plot arbitrary functions defined on surfaces, e.g. the Gauss map or functions indicating force or tension, offering various applications in science and visualization.

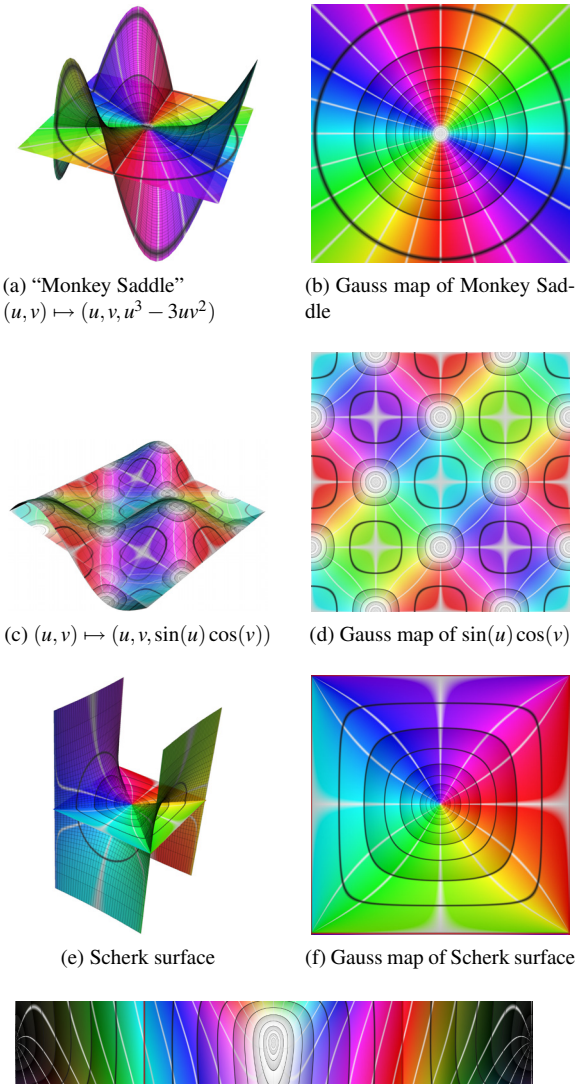

(a) "Monkey Saddle" $(u,v) \mapsto (u,v,u^3-3uv^2)$

(b) Gauss map of Monkey Saddle

(c) $(u,v) \mapsto (u,v,\sin(u)\cos(v))$

(d) Gauss map of $\sin(u)\cos(v)$

(e) Scherk surface

(f) Gauss map of Scherk surface

(g) Gauss map of Möbius strip

Figure 13: Domain colored Gauss maps

References

[Arn] ARNOLD D. N.: Graphics for complex analysis. http://www.ima.umn.edu/~arnold/complex.html.

[Ban] BANCHOFF T. F.: Complex function graphs. http://www.math.brown.edu/~banchoff/gc/script/CFGInd.html.

[Ben] BENNETT A. G.: Complex function grapher. http://www.math.ksu.edu/~bennett/jomacg/.

[dS] DA SILVA E. L.: Reviews of functions of one complex variable graphical representation from software development for learning support. http://sorzal-df.fc.unesp.br/~edvaldo/en/index.htm.

[Far] FARRIS F. A.: Visualizing complex-valued functions in the plane. http://www.maa.org/pubs/amm_complements/complex.html.

[Hla] HLAVACEK J.: Complex domain coloring. http://www6.svsu.edu/~jhlavace/Complex_Domain_Coloring/index.html.

[Lun04] LUNDMARK H.: Visualizing complex analytic functions using domain coloring. http://www.mai.liu.se/~halun/complex/domain_coloring-unicode.html, 2004.

[Nee97] NEEDHAM T.: *Visual Complex Analysis*. Oxford University Press, 1997.

[Per] PERGLER M.: Newton's method, julia and mandelbrot sets, and complex coloring. http://users.arczip.com/pergler/mp/documents/ptr/.

[Tha98] THALLER B.: Visualization of complex functions. *The Mathematica Journal 7* (1998).